EUROPEAN ORGANIZATION FOR NUCLEAR RESEARCH

CERN–EP/99–58

16 April 1999

Search for the Higgs boson in events with isolated photons at LEP II

DELPHI Collaboration

Abstract

A search for the Higgs boson in final states with one, two or three isolated photons has been performed based on data taken at LEP II by the DELPHI detector. The data analysed correspond to a total integrated luminosity of 67.5 pb^{-1} at centre-of-mass energies of 161 GeV (9.7 pb^{-1}), 172 GeV (10.1 pb^{-1}) and 183 GeV (47.7 pb^{-1}). No evidence for the processes $e^+e^- \to H\gamma$ with $H \to b\bar{b}$ or $\gamma\gamma$ and $e^+e^- \to Hq\bar{q}$ with $H \to \gamma\gamma$ was observed. Model-independent limits on $\sigma(e^+e^- \to H\gamma) \times BR(H \to b\bar{b})$, $\sigma(e^+e^- \to Hq\bar{q}) \times BR(H \to \gamma\gamma)$ and $\sigma(e^+e^- \to H\gamma) \times BR(H \to \gamma\gamma)$ are set, as well as model-dependent limits on Higgs boson anomalous couplings to vector bosons.

(Submitted to Physics Letters B)

P.Abreu[21], W.Adam[50], T.Adye[36], P.Adzic[11], I.Ajinenko[42], Z.Albrecht[17], T.Alderweireld[2], G.D.Alekseev[16], R.Alemany[49], T.Allmendinger[17], P.P.Allport[22], S.Almehed[24], U.Amaldi[9], N.Amapane[45], S.Amato[47], E.G.Anassontzis[3], P.Andersson[44], A.Andreazza[9], S.Andringa[21], P.Antilogus[25], W-D.Apel[17], Y.Arnoud[9], B.Åsman[44], J-E.Augustin[25], A.Augustinus[9], P.Baillon[9], P.Bambade[19], F.Barao[21], G.Barbiellini[46], R.Barbier[25], D.Y.Bardin[16], G.Barker[17], A.Baroncelli[38], M.Battaglia[15], M.Baubillier[23], K-H.Becks[52], M.Begalli[6], A.Behrmann[52], P.Beilliere[8], Yu.Belokopytov[9,53], N.C.Benekos[31], A.C.Benvenuti[5], C.Berat[14], M.Berggren[25], D.Bertini[25], D.Bertrand[2], M.Besancon[39], M.Bigi[45], M.S.Bilenky[16], M-A.Bizouard[19], D.Bloch[10], H.M.Blom[30], M.Bonesini[27], W.Bonivento[27], M.Boonekamp[39], P.S.L.Booth[22], A.W.Borgland[4], G.Borisov[19], C.Bosio[41], O.Botner[48], E.Boudinov[30], B.Bouquet[19], C.Bourdarios[19], T.J.V.Bowcock[22], I.Boyko[16], I.Bozovic[11], M.Bozzo[13], P.Branchini[38], T.Brenke[52], R.A.Brenner[48], P.Bruckman[18], J-M.Brunet[8], L.Bugge[32], T.Buran[32], T.Burgsmueller[52], B.Buschbeck[50], P.Buschmann[52], S.Cabrera[49], M.Caccia[27], M.Calvi[27], T.Camporesi[9], V.Canale[37], F.Carena[9], L.Carroll[22], C.Caso[13], M.V.Castillo Gimenez[49], A.Cattai[9], F.R.Cavallo[5], V.Chabaud[9], Ph.Charpentier[9], L.Chaussard[25], P.Checchia[35], G.A.Chelkov[16], R.Chierici[45], P.Chliapnikov[42], P.Chochula[7], V.Chorowicz[25], J.Chudoba[29], K.Cieslik[18], P.Collins[9], R.Contri[13], E.Cortina[49], G.Cosme[19], F.Cossutti[9], J-H.Cowell[22], H.B.Crawley[1], D.Crennell[36], S.Crepe[14], G.Crosetti[13], J.Cuevas Maestro[33], S.Czellar[15], M.Davenport[9], W.Da Silva[23], A.Deghorain[2], G.Della Ricca[46], P.Delpierre[26], N.Demaria[9], A.De Angelis[9], W.De Boer[17], C.De Clercq[2], B.De Lotto[46], A.De Min[35], L.De Paula[47], H.Dijkstra[9], L.Di Ciaccio[37,9], J.Dolbeau[8], K.Doroba[51], M.Dracos[10], J.Drees[52], M.Dris[31], A.Duperrin[25], J-D.Durand[9], G.Eigen[4], T.Ekelof[48], G.Ekspong[44], M.Ellert[48], M.Elsing[9], J-P.Engel[10], B.Erzen[43], M.Espirito Santo[21], E.Falk[24], G.Fanourakis[11], D.Fassouliotis[11], J.Fayot[23], M.Feindt[17], P.Ferrari[27], A.Ferrer[49], E.Ferrer-Ribas[19], F.Ferro[13], S.Fichet[23], A.Firestone[1], U.Flagmeyer[52], H.Foeth[9], E.Fokitis[31], F.Fontanelli[13], B.Franek[36], A.G.Frodesen[4], R.Fruhwirth[50], F.Fulda-Quenzer[19], J.Fuster[49], A.Galloni[22], D.Gamba[45], S.Gamblin[19], M.Gandelman[47], C.Garcia[49], C.Gaspar[9], M.Gaspar[47], U.Gasparini[35], Ph.Gavillet[9], E.N.Gazis[31], D.Gele[10], L.Gerdyukov[42], N.Ghodbane[25], I.Gil[49], F.Glege[52], R.Gokieli[9,51], B.Golob[43], G.Gomez-Ceballos[40], P.Goncalves[21], I.Gonzalez Caballero[40], G.Gopal[36], L.Gorn[1,54], M.Gorski[51], Yu.Gouz[42], V.Gracco[13], J.Grahl[1], E.Graziani[38], C.Green[22], H-J.Grimm[17], P.Gris[39], G.Grosdidier[19], K.Grzelak[51], M.Gunther[48], J.Guy[36], F.Hahn[9], S.Hahn[52], S.Haider[9], A.Hallgren[48], K.Hamacher[52], J.Hansen[32], F.J.Harris[34], V.Hedberg[24], S.Heising[17], J.J.Hernandez[49], P.Herquet[2], H.Herr[9], T.L.Hessing[34], J.-M.Heuser[52], E.Higon[49], S-O.Holmgren[44], P.J.Holt[34], S.Hoorelbeke[2], M.Houlden[22], J.Hrubec[50], K.Huet[2], G.J.Hughes[22], K.Hultqvist[44], J.N.Jackson[22], R.Jacobsson[9], P.Jalocha[9], R.Janik[7], Ch.Jarlskog[24], G.Jarlskog[24], P.Jarry[39], B.Jean-Marie[19], E.K.Johansson[44], P.Jonsson[25], C.Joram[9], P.Juillot[10], F.Kapusta[23], K.Karafasoulis[11], S.Katsanevas[25], E.C.Katsoufis[31], R.Keranen[17], B.P.Kersevan[43], B.A.Khomenko[16], N.N.Khovanski[16], A.Kiiskinen[15], B.King[22], A.Kinvig[22], N.J.Kjaer[30], O.Klapp[52], H.Klein[9], P.Kluit[30], P.Kokkinias[11], M.Koratzinos[9], V.Kostioukhine[42], C.Kourkoumelis[3], O.Kouznetsov[39], M.Krammer[50], E.Kriznic[43], J.Krstic[11], Z.Krumstein[16], P.Kubinec[7], J.Kurowska[51], K.Kurvinen[15], J.W.Lamsa[1], D.W.Lane[1], P.Langefeld[52], V.Lapin[42], J-P.Laugier[39], R.Lauhakangas[15], G.Leder[50], F.Ledroit[14], V.Lefebure[2], L.Leinonen[44], A.Leisos[11], R.Leitner[29], J.Lemonne[2], G.Lenzen[52], V.Lepeltier[19], T.Lesiak[18], M.Lethuillier[39], J.Libby[34], D.Liko[9], A.Lipniacka[44], I.Lippi[35], B.Loerstad[24], J.G.Loken[34], J.H.Lopes[47], J.M.Lopez[40], R.Lopez-Fernandez[14], D.Loukas[11], P.Lutz[39], L.Lyons[34], J.MacNaughton[50], J.R.Mahon[6], A.Maio[21], A.Malek[52], T.G.M.Malmgren[44], S.Maltezos[31], V.Malychev[16], F.Mandl[50], J.Marco[40], R.Marco[40], B.Marechal[47], M.Margoni[35], J-C.Marin[9], C.Mariotti[9], A.Markou[11], C.Martinez-Rivero[19], F.Martinez-Vidal[49], S.Marti i Garcia[9], J.Masik[12], N.Mastroyiannopoulos[11], F.Matorras[40], C.Matteuzzi[27], G.Matthiae[37], F.Mazzucato[35], M.Mazzucato[35], M.Mc Cubbin[22], R.Mc Kay[1], R.Mc Nulty[22], G.Mc Pherson[22], C.Meroni[27], W.T.Meyer[1], A.Miagkov[42], E.Migliore[45], L.Mirabito[25], W.A.Mitaroff[50], U.Mjoernmark[24], T.Moa[44], M.Moch[17], R.Moeller[28], K.Moenig[9], M.R.Monge[13], X.Moreau[23], P.Morettini[13], G.Morton[34], U.Mueller[52], K.Muenich[52], M.Mulders[30], C.Mulet-Marquis[14], R.Muresan[24], W.J.Murray[36], B.Muryn[14,18], G.Myatt[34], T.Myklebust[32], F.Naraghi[14], M.Nassiakou[11], F.L.Navarria[5], S.Navas[49], K.Nawrocki[51], P.Negri[27], S.Nemecek[12], N.Neufeld[9], R.Nicolaidou[39], B.S.Nielsen[28], M.Nikolenko[10,16], V.Nomokonov[15], A.Normand[22], A.Nygren[24], V.Obraztsov[42], A.G.Olshevski[16], A.Onofre[21], R.Orava[15], G.Orazi[10], K.Osterberg[15], A.Ouraou[39], M.Paganoni[27], S.Paiano[5], R.Pain[23], R.Paiva[21], J.Palacios[34], H.Palka[18], Th.D.Papadopoulou[31,9], K.Papageorgiou[11], L.Pape[9], C.Parkes[9], F.Parodi[13], U.Parzefall[22], A.Passeri[38], O.Passon[52], M.Pegoraro[35], L.Peralta[21], M.Pernicka[50], A.Perrotta[5], C.Petridou[46], A.Petrolini[13], H.T.Phillips[36], F.Pierre[39], M.Pimenta[21], E.Piotto[27], T.Podobnik[43], M.E.Pol[6], G.Polok[18], P.Poropat[46], V.Pozdniakov[16], P.Privitera[37], N.Pukhaeva[16], A.Pullia[27], D.Radojicic[34], S.Ragazzi[27], H.Rahmani[31], P.N.Ratoff[20], A.L.Read[32], P.Rebecchi[9], N.G.Redaelli[27], M.Regler[50], D.Reid[30], R.Reinhardt[52], P.B.Renton[34], L.K.Resvanis[3], F.Richard[19], J.Ridky[12], G.Rinaudo[45], O.Rohne[32], A.Romero[45], P.Ronchese[35], E.I.Rosenberg[1], P.Rosinsky[7], P.Roudeau[19], T.Rovelli[5], Ch.Royon[39], V.Ruhlmann-Kleider[39], A.Ruiz[40], H.Saarikko[15], Y.Sacquin[39], A.Sadovsky[16], G.Sajot[14], J.Salt[49], D.Sampsonidis[11], M.Sannino[13], H.Schneider[17], Ph.Schwemling[23], B.Schwering[52], U.Schwickerath[17], M.A.E.Schyns[52], F.Scuri[46], P.Seager[20], Y.Sedykh[16], A.M.Segar[34], R.Sekulin[36], R.C.Shellard[6], A.Sheridan[22], M.Siebel[52], L.Simard[39], F.Simonetto[35], A.N.Sisakian[16], G.Smadja[25], O.Smirnova[24], G.R.Smith[36], O.Solovianov[42], A.Sopczak[17], R.Sosnowski[51], T.Spassov[21], E.Spiriti[38], P.Sponholz[52], S.Squarcia[13], C.Stanescu[38], S.Stanic[43], K.Stevenson[34], A.Stocchi[19], J.Strauss[50], R.Strub[10], B.Stugu[4], M.Szczekowski[51], M.Szeptycka[51], T.Tabarelli[27], O.Tchikilev[42], F.Tegenfeldt[48], F.Terranova[27], J.Thomas[34], J.Timmermans[30], N.Tinti[5], L.G.Tkatchev[16],

S.Todorova[10], A.Tomaradze[2], B.Tome[21], A.Tonazzo[9], L.Tortora[38], G.Transtromer[24], D.Treille[9], G.Tristram[8], M.Trochimczuk[51], C.Troncon[27], A.Tsirou[9], M-L.Turluer[39], I.A.Tyapkin[16], S.Tzamarias[11], O.Ullaland[9], V.Uvarov[42], G.Valenti[5], E.Vallazza[46], G.W.Van Apeldoorn[30], P.Van Dam[30], W.K.Van Doninck[2], J.Van Eldik[30], A.Van Lysebetten[2], N.Van Remortel[2], I.Van Vulpen[30], N.Vassilopoulos[34], G.Vegni[27], L.Ventura[35], W.Venus[36,9], F.Verbeure[2], M.Verlato[35], L.S.Vertogradov[16], V.Verzi[37], D.Vilanova[39], L.Vitale[46], E.Vlasov[42], A.S.Vodopyanov[16], C.Vollmer[17], G.Voulgaris[3], V.Vrba[12], H.Wahlen[52], C.Walck[44], C.Weiser[17], D.Wicke[52], J.H.Wickens[2], G.R.Wilkinson[9], M.Winter[10], M.Witek[18], G.Wolf[9], J.Yi[1], O.Yushchenko[42], A.Zalewska[18], P.Zalewski[51], D.Zavrtanik[43], E.Zevgolatakos[11], N.I.Zimin[16,24], G.C.Zucchelli[44], G.Zumerle[35]

[1] Department of Physics and Astronomy, Iowa State University, Ames IA 50011-3160, USA
[2] Physics Department, Univ. Instelling Antwerpen, Universiteitsplein 1, BE-2610 Wilrijk, Belgium
and IIHE, ULB-VUB, Pleinlaan 2, BE-1050 Brussels, Belgium
and Faculté des Sciences, Univ. de l'Etat Mons, Av. Maistriau 19, BE-7000 Mons, Belgium
[3] Physics Laboratory, University of Athens, Solonos Str. 104, GR-10680 Athens, Greece
[4] Department of Physics, University of Bergen, Allégaten 55, NO-5007 Bergen, Norway
[5] Dipartimento di Fisica, Università di Bologna and INFN, Via Irnerio 46, IT-40126 Bologna, Italy
[6] Centro Brasileiro de Pesquisas Físicas, rua Xavier Sigaud 150, BR-22290 Rio de Janeiro, Brazil
and Depto. de Física, Pont. Univ. Católica, C.P. 38071 BR-22453 Rio de Janeiro, Brazil
and Inst. de Física, Univ. Estadual do Rio de Janeiro, rua São Francisco Xavier 524, Rio de Janeiro, Brazil
[7] Comenius University, Faculty of Mathematics and Physics, Mlynska Dolina, SK-84215 Bratislava, Slovakia
[8] Collège de France, Lab. de Physique Corpusculaire, IN2P3-CNRS, FR-75231 Paris Cedex 05, France
[9] CERN, CH-1211 Geneva 23, Switzerland
[10] Institut de Recherches Subatomiques, IN2P3 - CNRS/ULP - BP20, FR-67037 Strasbourg Cedex, France
[11] Institute of Nuclear Physics, N.C.S.R. Demokritos, P.O. Box 60228, GR-15310 Athens, Greece
[12] FZU, Inst. of Phys. of the C.A.S. High Energy Physics Division, Na Slovance 2, CZ-180 40, Praha 8, Czech Republic
[13] Dipartimento di Fisica, Università di Genova and INFN, Via Dodecaneso 33, IT-16146 Genova, Italy
[14] Institut des Sciences Nucléaires, IN2P3-CNRS, Université de Grenoble 1, FR-38026 Grenoble Cedex, France
[15] Helsinki Institute of Physics, HIP, P.O. Box 9, FI-00014 Helsinki, Finland
[16] Joint Institute for Nuclear Research, Dubna, Head Post Office, P.O. Box 79, RU-101 000 Moscow, Russian Federation
[17] Institut für Experimentelle Kernphysik, Universität Karlsruhe, Postfach 6980, DE-76128 Karlsruhe, Germany
[18] Institute of Nuclear Physics and University of Mining and Metalurgy, Ul. Kawiory 26a, PL-30055 Krakow, Poland
[19] Université de Paris-Sud, Lab. de l'Accélérateur Linéaire, IN2P3-CNRS, Bât. 200, FR-91405 Orsay Cedex, France
[20] School of Physics and Chemistry, University of Lancaster, Lancaster LA1 4YB, UK
[21] LIP, IST, FCUL - Av. Elias Garcia, 14-1°, PT-1000 Lisboa Codex, Portugal
[22] Department of Physics, University of Liverpool, P.O. Box 147, Liverpool L69 3BX, UK
[23] LPNHE, IN2P3-CNRS, Univ. Paris VI et VII, Tour 33 (RdC), 4 place Jussieu, FR-75252 Paris Cedex 05, France
[24] Department of Physics, University of Lund, Sölvegatan 14, SE-223 63 Lund, Sweden
[25] Université Claude Bernard de Lyon, IPNL, IN2P3-CNRS, FR-69622 Villeurbanne Cedex, France
[26] Univ. d'Aix - Marseille II - CPP, IN2P3-CNRS, FR-13288 Marseille Cedex 09, France
[27] Dipartimento di Fisica, Università di Milano and INFN, Via Celoria 16, IT-20133 Milan, Italy
[28] Niels Bohr Institute, Blegdamsvej 17, DK-2100 Copenhagen Ø, Denmark
[29] NC, Nuclear Centre of MFF, Charles University, Areal MFF, V Holesovickach 2, CZ-180 00, Praha 8, Czech Republic
[30] NIKHEF, Postbus 41882, NL-1009 DB Amsterdam, The Netherlands
[31] National Technical University, Physics Department, Zografou Campus, GR-15773 Athens, Greece
[32] Physics Department, University of Oslo, Blindern, NO-1000 Oslo 3, Norway
[33] Dpto. Fisica, Univ. Oviedo, Avda. Calvo Sotelo s/n, ES-33007 Oviedo, Spain
[34] Department of Physics, University of Oxford, Keble Road, Oxford OX1 3RH, UK
[35] Dipartimento di Fisica, Università di Padova and INFN, Via Marzolo 8, IT-35131 Padua, Italy
[36] Rutherford Appleton Laboratory, Chilton, Didcot OX11 OQX, UK
[37] Dipartimento di Fisica, Università di Roma II and INFN, Tor Vergata, IT-00173 Rome, Italy
[38] Dipartimento di Fisica, Università di Roma III and INFN, Via della Vasca Navale 84, IT-00146 Rome, Italy
[39] DAPNIA/Service de Physique des Particules, CEA-Saclay, FR-91191 Gif-sur-Yvette Cedex, France
[40] Instituto de Fisica de Cantabria (CSIC-UC), Avda. los Castros s/n, ES-39006 Santander, Spain
[41] Dipartimento di Fisica, Università degli Studi di Roma La Sapienza, Piazzale Aldo Moro 2, IT-00185 Rome, Italy
[42] Inst. for High Energy Physics, Serpukov P.O. Box 35, Protvino, (Moscow Region), Russian Federation
[43] J. Stefan Institute, Jamova 39, SI-1000 Ljubljana, Slovenia and Laboratory for Astroparticle Physics,
Nova Gorica Polytechnic, Kostanjeviska 16a, SI-5000 Nova Gorica, Slovenia,
and Department of Physics, University of Ljubljana, SI-1000 Ljubljana, Slovenia
[44] Fysikum, Stockholm University, Box 6730, SE-113 85 Stockholm, Sweden
[45] Dipartimento di Fisica Sperimentale, Università di Torino and INFN, Via P. Giuria 1, IT-10125 Turin, Italy
[46] Dipartimento di Fisica, Università di Trieste and INFN, Via A. Valerio 2, IT-34127 Trieste, Italy
and Istituto di Fisica, Università di Udine, IT-33100 Udine, Italy
[47] Univ. Federal do Rio de Janeiro, C.P. 68528 Cidade Univ., Ilha do Fundão BR-21945-970 Rio de Janeiro, Brazil
[48] Department of Radiation Sciences, University of Uppsala, P.O. Box 535, SE-751 21 Uppsala, Sweden
[49] IFIC, Valencia-CSIC, and D.F.A.M.N., U. de Valencia, Avda. Dr. Moliner 50, ES-46100 Burjassot (Valencia), Spain
[50] Institut für Hochenergiephysik, Österr. Akad. d. Wissensch., Nikolsdorfergasse 18, AT-1050 Vienna, Austria
[51] Inst. Nuclear Studies and University of Warsaw, Ul. Hoza 69, PL-00681 Warsaw, Poland
[52] Fachbereich Physik, University of Wuppertal, Postfach 100 127, DE-42097 Wuppertal, Germany
[53] On leave of absence from IHEP Serpukhov
[54] Now at University of Florida

1 Introduction

The Standard Model (SM) has been successful in describing the interactions between the gauge bosons and the fermions. Direct tests of the self-interactions of the electroweak gauge bosons are being carried out at LEP II and the Tevatron and no deviations from the SM have been observed so far. In the symmetry breaking sector the picture is quite different. There is no direct experimental evidence for the couplings of the gauge bosons to the Higgs boson and extensions of the symmetry breaking sector of the SM are still possible. These extensions can be described in terms of an effective Lagrangian density, which could give rise to anomalous $H\gamma\gamma$ and $HZ\gamma$ couplings [1].

In the SM the HZγ and H$\gamma\gamma$ vertices do not exist. The Z$^*/\gamma^* \rightarrow$Hγ and H$\rightarrow \gamma\gamma$ processes must involve charged particle loops and therefore the corresponding cross-sections are tiny. For example, in the SM the total cross-section for $e^+e^- \rightarrow H\gamma$ at LEP II energies varies from 0.2 to 0.02 fb for the Higgs boson's mass in the range $70 < M_H < 150\ GeV/c^2$ [2,3], and the branching ratio BR(H$\rightarrow \gamma\gamma$) is of order 10^{-3} [4]. The presence of new particles in the loops (as predicted, for instance, in the Minimal Supersymmetric Standard Model) would not increase the strength of the couplings by more than a factor of three [5,6]. On the other hand, the existence of anomalous HZγ and H$\gamma\gamma$ couplings in the framework of the Standard Model symmetry group could result in the enhancement of the $e^+e^- \rightarrow H\gamma$ cross-section and of the $H \rightarrow \gamma\gamma$ decay rate by two or three orders of magnitude [1,7], thus allowing these processes to be detectable at LEP II.

A search for a Higgs boson in final states with one, two or three isolated photons has been performed on the data taken at LEP II by the DELPHI detector. More precisely, the topologies investigated correspond to the processes $e^+e^- \rightarrow H\gamma$ with $H \rightarrow b\bar{b}$ or $\gamma\gamma$ and to the process $e^+e^- \rightarrow Hq\bar{q}$ with $H \rightarrow \gamma\gamma$. The number of candidates found are compatible with the background expectation. Model-independent limits on $\sigma(e^+e^- \rightarrow H\gamma) \times BR(H \rightarrow b\bar{b})$, $\sigma(e^+e^- \rightarrow Hq\bar{q}) \times BR(H \rightarrow \gamma\gamma)$ and $\sigma(e^+e^- \rightarrow H\gamma) \times BR(H \rightarrow \gamma\gamma)$ are set. Although these processes are highly suppressed in the SM, they can be used to search for anomalous couplings of the Higgs boson to photons and to the Z [1,7]. This study was also carried out.

The data were taken at centre-of-mass energies of 161 GeV, 172 GeV, and 183 GeV with integrated luminosities of 9.7 pb^{-1}, 10.1 pb^{-1} and 47.7 pb^{-1} respectively. The effects of experimental resolution, both on the signals and on backgrounds, were studied by generating Monte Carlo events for the possible signals and for the SM processes and passing them through the full DELPHI simulation chain. Other limits on $\sigma(e^+e^- \rightarrow Hq\bar{q}) \times BR(H \rightarrow \gamma\gamma)$ from a LEP experiment can be found in [8]. A detailed description of the DELPHI detector and its performance can be found elsewhere [9,10].

2 Production and decay of the Higgs boson

The Standard Model (SM) predicts the existence of one neutral Higgs boson H [11] which is searched for at LEP. Direct Higgs boson production in e^+e^- collisions is possible (figure 1(a)), but since the coupling of the Higgs boson to the fermions is proportional to their squared masses [12], this process has a very small cross-section. Therefore, at LEP the Higgs boson has been mainly sought through the process $e^+e^- \rightarrow HZ^*$. In the Standard Model for Higgs boson masses, M_H, up to 120 GeV/c^2 [13], the main H decay process is through $b\bar{b}$. Several possible channels of Z* decay have been analysed and lower limits for M_H have been set by the LEP collaborations [14].

Although suppressed in the framework of the SM, final states with one, two or three photons have been proposed as possible clear signatures for the discovery of the Higgs boson [2,3]. These final states can occur through:

$$e^+e^- \to H\gamma \to b\bar{b}\gamma \tag{1}$$
$$e^+e^- \to Hq\bar{q} \to \gamma\gamma q\bar{q} \tag{2}$$
$$e^+e^- \to H\gamma \to \gamma\gamma\gamma. \tag{3}$$

In (1) and (3) a mono-energetic photon recoils against the Higgs boson, giving rise to a resonance in the photon spectrum, albeit with a combinatorial background in (3). The main background to process (1) is $Z\gamma \to q\bar{q}\gamma$. In (2) the polar angle distributions of the two photons are mainly isotropic, while the main background consists of double ISR photons in $q\bar{q}$ events which have a forward peaked distribution. Selection criteria on the polar angle can thus be applied to separate the signal from the background. Final states from (3) are characterised by three energetic photons. The QED background to this process has at least one forward soft photon, which again provides a good discrimination between signal and background.

Within the Standard Model, reactions (1), (2) and (3) occur through W or charged fermions loops. The amplitude is dominated by the W loop contribution [3] and is negligible for LEP energies and luminosities [1,3,15,16]. A possible enhancement of the production and decay rates of the Higgs boson can be originated by anomalous couplings of the Higgs boson to the vector bosons. These interactions can be expressed in terms of effective energy-dimension-six operators included in the interaction Lagrangian density [1]:

$$\mathcal{L}_{eff} = \sum_{i=1}^{7} \frac{f_i}{\Lambda^2} O_i, \tag{4}$$

where the O_i are the operators which represent the anomalous couplings, Λ is the typical energy scale of the interaction and f_i are the constants which define the strength of each term. One of the anomalous operators in equation (4) contributes via the renormalization of the Higgs wave function, giving rise to a common rescaling of all Higgs production and decay rates [1] – this constant factor was set to one. The other six operators give rise to the anomalous couplings H$\gamma\gamma$, HZγ, HZZ and HWW, which can be written in the unitary gauge as [1,7]:

$$\begin{aligned}
\mathcal{L}_{eff}^{HVV} &= g\frac{m_W}{\Lambda^2}\,[\, -\frac{s^2(f_{BB}+f_{WW}-f_{BW})}{2} H A_{\mu\nu}A^{\mu\nu} + \frac{2m_W^2}{g^2}\frac{f_{\phi,1}}{c^2} H Z_\mu Z^\mu \\
&+ \frac{c^2 f_W + s^2 f_B}{2c^2} Z_{\mu\nu} Z^\mu (\partial^\nu H) - \frac{s^4 f_{BB} + c^4 f_{WW} + s^2c^2 f_{BW}}{2c^2} H Z_{\mu\nu} Z^{\mu\nu} \\
&+ \frac{s(f_W - f_B)}{2c} A_{\mu\nu} Z^\mu (\partial^\nu H) + \frac{s(2s^2 f_{BB} - 2c^2 f_{WW} + (c^2-s^2) f_{BW})}{2c} H A_{\mu\nu} Z^{\mu\nu} \\
&+ \frac{f_W}{2}(W^+_{\mu\nu} W^{-\mu} + W^-_{\mu\nu} W^{+\mu})(\partial^\nu H) - f_{WW} H W^+_{\mu\nu} W^{-\mu\nu}\,]\,,
\end{aligned} \tag{5}$$

where $g^2 = e^2/s^2 = 8m_W^2 G_F/\sqrt{2}$, $s(c)$=sin(cos)θ_W, G_F is the Fermi coupling constant, m_W the W boson's mass, θ_W the weak mixing angle and $X_{\mu\nu} = \partial_\mu X_\nu - \partial_\nu X_\mu$ with $X = A, Z, W$, the photon, Z and W fields respectively.

The most remarkable feature of the effective Lagrangian is the existence of direct HZγ and H$\gamma\gamma$ couplings, resulting in possible large deviations from the SM cross-sections of the studied processes. The production of the Higgs boson associated with photons would then increase and $H \to \gamma\gamma$, which has a very small branching ratio in the SM, might even become the dominant decay. A large enhancement of the $Z^* \to H\gamma$ decay width would mean that the $\frac{f_i}{\Lambda^2}$ coefficients were of the order $10 - 100\ TeV^{-2}$.

On the other hand, the introduction of $\mathcal{L}_{eff}$ (4) as an extension to the SM Lagrangian will also contribute to other processes besides the Higgs boson interactions, namely to gauge boson self-interactions [1]. Therefore, some of the $\frac{f_i}{\Lambda^2}$ coefficients are already bound by precise measurements of the SM parameters. The coefficient $f_{\phi,1}$ would contribute to a change of the Z mass and f_{BW} would change the $W^3 - B$ mixing and are thus bound by low energy experiments with typical values of $O(0.1 - 1\ TeV^{-2})$ [17]. The coefficients f_B and f_W contribute to the Trilinear Gauge boson Couplings (TGC), but these measurements still allow values of $O(100\ TeV^{-2})$. The remaining coefficients have no tight restrictions. Therefore, in what follows, the $f_{\phi,1}$ and f_{BW} coefficients will be taken as zero, and only f_B, f_W, f_{BB} and f_{WW} will be considered.

The Higgs boson production and decay processes where anomalous HZγ, HZZ and H$\gamma\gamma$ couplings are present at tree level, giving final states with one, two or three photons are displayed in figures 1(b) to 1(e). However, process 1(e) will not be taken into account in the present analyses, since it is negligible in most of the parameter space when compared to process 1(c).

Possible signals for processes (1), (2) and (3) were simulated using the PYTHIA generator [18]. Events were generated at a set of possible Higgs boson masses, ranging from 60 to 180 GeV/c^2.

The interpretation of the results requires the computation of the cross-sections as a function of the anomalous couplings, f_i/Λ^2, as well as of M_H (Higgs boson mass). The CompHEP package was used for this calculation [19]. All the new interactions were incorporated in the generator by the use of the LanHEP code [20]. In a scenario where the anomalous contributions to the cross-section are important, the Higgs boson width depends on the f_i values and must be supplied to CompHEP. The computation of the Higgs boson width was taken from [1] and [21] and includes the interference between the SM model contribution and the new anomalous diagrams. In the M_H range studied (from 60 to 180 GeV/c^2), decays of the Higgs boson into ZZ* or WW* are important [16] and their contribution was taken into account [21]. The Higgs boson width increases for higher values of the Higgs mass and for increasing absolute values of the anomalous couplings. It ranges from a few MeV up to hundreds of MeV, never reaching the experimental M_H resolution for the range of Higgs masses and couplings considered.

The main background to processes (1) and (2) are $Z \to q\bar{q}$ with initial and final state radiation. For process (3) the main background is the QED process $e^+e^- \to \gamma\gamma\gamma$. All the other relevant SM processes were also considered.

Bhabha events were generated with the Berends,Hollik and Kleiss generator [22], while $e^+e^- \to Z\gamma$ events were generated with PYTHIA [18]. PYTHIA was also used for the following processes: $e^+e^- \to WW$, $e^+e^- \to We\nu$, $e^+e^- \to ZZ$, and $e^+e^- \to Zee$. In all four-fermion channels, studies with the EXCALIBUR generator [23] were also performed. The two-photon ("$\gamma\gamma$") physics events were generated according to the TWOGAM [24] generator for quark channels and to the Berends, Daverveldt and Kleiss generator [25] for the Quark Parton Model giving hadrons. Compton events were generated according to [26], and $e^+e^- \to \gamma\gamma\gamma$ events according to [27].

3 Event selection

Charged particles were considered only if they had momentum greater than 0.1 GeV/c and impact parameters in the transverse plane and in the beam direction below 4 cm and 10 cm, respectively. Energy depositions in the calorimeters unassociated to charged particle tracks were required to be above 0.1 GeV.

Neutral clusters were classified as isolated photons if the total energy inside a double cone centered around the cluster with half angles of 5° and 15°, was less than 1 GeV and if there were no charged particles above 0.25 GeV/c inside the inner cone. The energy of the isolated photons was then reevaluated as the sum of the energies of all the particles inside the inner cone.

The final state topologies under study are characterized by the presence of jets and photons and the absence of isolated leptons. Therefore, the identification of isolated charged particles is of importance for vetoing isolated leptons. The algorithm used to identify isolated charged particles demanded that inside a double cone centered on the track, with internal and external half angles of 5° and 25°, the total charged energy was less than 1 GeV and the total neutral energy was less than 2 GeV. The energy of the particle was redefined as the sum of the energies of all the charged and neutral particles inside the inner cone and required to be greater than 4 GeV.

For the topology with three photons, no charged tracks were allowed in the event (no converted photons were recovered), the visible energy in the polar angle region between 20° and 160° was required to be above 0.1 $\sqrt{s}$, and the minimum energy of each photon was required to be 2 GeV. Whenever more than 3 GeV of hadronic energy was associated to a photon, at least 90 % of it had to be in the first layer of the Hadronic Calorimeter (HCAL).

Hadronic topologies ($b\bar{b}\gamma$ and $q\bar{q}\gamma\gamma$), required that at least six charged tracks were present as well as one or two electromagnetic clusters with energy greater than 5 GeV and visible energy in the polar angle region between 20° and 160° above 0.2 $\sqrt{s}$, including at least one charged particle with an energy greater than 5 GeV. No isolated charged particles were allowed. A protection against fake photons was set by requiring less than 1 GeV in the HCAL and no High Density Projection Chamber (HPC) layer with more than 90% of the photon electromagnetic energy. Alternatively an energy deposition in the hadronic calorimeter was allowed if at least 90% was in the first layer.

All selected charged particles and neutrals not associated to photons were forced to be clustered into jets using the DURHAM jet algorithm [28]. The algorithm was applied three times, requiring a defined number of jets, $N_{jets} = 1, 2, 3$. The values of the resolution variable at each transition, $y_{cut(N_{jets}+1 \to N_{jets})}$, characterize the event topology.

The hadronic final states searched for are well defined 2 jet topologies. Therefore, events with a clear monojet or 3 jet signature were excluded by constraining the resolution variables $y_{cut(2\to1)}$ to be greater than 0.003 and $y_{cut(3\to2)}$ to be smaller than 0.06. Events with 2 jets (and photons) were preselected if the jets had polar angle in the range 20° - 160° and momentum greater than 1 GeV/c.

The analyses were optimized for each topology and selection levels were established. Selection level 1 corresponds to adding topological requirements to the above set of selection criteria. After selection level 1, specific selection criteria were applied to the preselected samples corresponding to selection level 2. Selection level 3 is exclusively for the $b\bar{b}\gamma$ topology and consists of tagging the b quarks.

These selection criteria are described in subsections 3.1, 3.2 and 3.3 for the $b\bar{b}\gamma$, $q\bar{q}\gamma\gamma$ and $\gamma\gamma\gamma$ final states respectively. The comparison between the number of events found

in data and the Monte Carlo expectation for the various topologies and for the different selection levels is displayed in table 1. The average signal selection efficiency corresponding to the last selection level for each searched topology is displayed in table 2 for the three centre-of-mass energy values.

$\sqrt{s}(GeV)$	topology	selection level		
		1	2	3
161	$b\bar{b}\gamma$	136 (128±4)	37 (41±2)	4 (5±1)
	$q\bar{q}\gamma\gamma$	22 (14±1)	0 (2.0±0.5)	-
	$\gamma\gamma\gamma$	55 (56±1)	1 (0.7±0.1)	-
172	$b\bar{b}\gamma$	109 (103±3)	37 (36±2)	7 (6±1)
	$q\bar{q}\gamma\gamma$	13 (12±1)	0 (1.0±0.3)	-
	$\gamma\gamma\gamma$	41 (38±1)	1 (0.5±0.1)	-
183	$b\bar{b}\gamma$	412 (418±7)	114 (141±4)	21 (23±2)
	$q\bar{q}\gamma\gamma$	57 (57±3)	7 (5±1)	-
	$\gamma\gamma\gamma$	189 (217±4)	1 (2.0±0.2)	-

Table 1: Number of events passing the sets of cuts corresponding to the selection levels described in the text for each topology and centre-of-mass energy. The MC predicted numbers of events and their statistical errors, are displayed within parentheses. Selection level 3 applies only to the $b\bar{b}\gamma$ topology.

$\sqrt{s}$(GeV)	161			172			183		
topology	$b\bar{b}\gamma$	$q\bar{q}\gamma\gamma$	$\gamma\gamma\gamma$	$b\bar{b}\gamma$	$q\bar{q}\gamma\gamma$	$\gamma\gamma\gamma$	$b\bar{b}\gamma$	$q\bar{q}\gamma\gamma$	$\gamma\gamma\gamma$
ϵ	35%	24%	33%	39%	27%	33%	37%	26%	34%

Table 2: Average signal selection efficiencies at the final selection level for the three searched topologies and for the different centre-of-mass energy values.

An important contribution to the signal selection efficiencies comes from the photon reconstruction efficiency. The $\gamma\gamma(\gamma)$ QED simulation was used to perform a systematic study of the efficiency of the isolated photon reconstruction algorithm described previously. This efficiency was found to be 90% in the barrel region (polar angle between 42° and 138°) of DELPHI and 70% in the part of the forward region considered in the analyses (polar angle between 25° and 35° or between 145° and 155°).

The presence of matter in front of the electromagnetic calorimeters is a source of a non-negligible photon conversion rate. The probability that a photon would convert in the tracking detectors and be reconstructed was evaluated for the polar angle regions considered in the analyses. This was done using both a $\gamma\gamma$ sample selected from the 183 GeV data and the respective $\gamma\gamma(\gamma)$ QED full simulation. Within statistics, a reasonable agreement between data and simulation was found. The systematic uncertainty due to the material description in the simulation was found to be negligible compared to that from data statistics.

3.1 Events with one photon and two jets

Selection criteria were implemented to identify events with two jets and only one isolated photon. Candidates were required to have the isolated photon with polar angle between 10° and 170° (level 1).

After these cuts the following selection criteria were applied to the data

- photon angle to the nearest jet direction, greater than 25°;
- photon momentum greater than 20 GeV/c;
- photon polar angle between 40° and 140°.

In order to improve momentum and energy resolution, a three body kinematic fit [29] imposing total energy and momentum conservation was performed on the selected events. Only events with a χ^2 per degree of freedom lower than 5 were accepted (level 2); the jet-jet effective mass resolution was then 3 GeV/c^2.

Figure 2(a) shows the jet-jet invariant mass distribution at 183 GeV after the kinematic fit. The peak of the radiative return to the Z is reconstructed with a good resolution. The mass distribution of a simulated signal at 70 GeV/c^2 is also shown.

The main decay channel for the Higgs boson in the studied mass range is through $b\bar{b}$. In order to reduce the $q\bar{q}\gamma$ background, event flavour tagging was performed based on the identification of the final state quark. The b-tagging probability is shown in figure 2(b) for the 183 GeV data, for the expected background and for a simulated Higgs signal of 70 GeV/c^2. Events with a high probability of containing a b quark (b-tag variable, as defined in references [10] and [30], lower than 0.001) were accepted (level 3). The efficiency for this b-tagging selection was 70% and the purity of the data sample was estimated to be 86%.

3.2 Events with two photons and two jets

Selection criteria were used to identify events with two jets and two isolated photons (level 1). A four body kinematic fit [29] was performed on the selected sample imposing total energy and momentum conservation. Only events with χ^2 per degree of freedom less than 5 were accepted corresponding to a mass resolution of 4 GeV for the Higgs signal.

The $\gamma\gamma$ and jet-jet invariant mass distributions after this fit at $\sqrt{s}$ = 183 GeV are displayed in figure 3. The corresponding reconstructed mass spectrum for a 70 GeV/c^2 Higgs boson signal is also shown. After the fit the following cuts were imposed (level 2):

- fitted photon polar angles between 20° and 160° ;
- angle between photons greater than 80°.

3.3 Events with three photons

Selection criteria were implemented to identify events with three isolated photons. Each of the photon candidates was required to fulfill the following criteria:

- There could not be any Vertex Detector (VD) track element pointing to the photon within 2° (6°) in azimuthal angle in the barrel (forward) region of DELPHI (a VD track element was defined as at least two hits in different VD layers aligned within an azimuthal angle interval of 0.5°).

- If the photon candidate was located inside the FEMC (Forward ElectroMagnetic Calorimeter):
  - Its polar angle had to be greater than 25° and less than 35° or greater than 145° and less than 155°;
  - Its associated hadronic energy had to be less than 15% of its total deposited energy.
- If the photon candidate was inside the HPC then :
  - Its polar angle had to be greater than 42° and less than 88° or greater than 92° and less than 138°;
  - If its azimuthal angle lay outside the inter-modular divisions [1], there had to be at least three HPC layers with more than 5% of the total electromagnetic energy of the photon candidate.

The preselected $\gamma\gamma\gamma$ sample(level 1) consisted of events with at least two photons fulfilling the above criteria. Moreover, the two most energetic photons had to have energies above 15% of the collision energy and to be separated by more than 30°.

The preselected samples correspond to a broad selection of $\gamma\gamma(\gamma)$ QED events. A dedicated analysis of this process including the 161, 172 and 183 GeV data sets can be found in [31].

The second level of the event selection consisted in demanding a third photon (within the above conditions) with energy above 6% of the collision energy. The energies can be rescaled by imposing energy and momentum conservation and using the measured polar and azimuthal angles. The compatibility of the momenta calculated from the angles with the measured momenta was quantified on a χ^2 basis [2]. After the event selection, a three-body kinematic fit [32] was applied to the data sample and all selected events were found to be compatible with a $\chi^2 < 3$. The invariant masses of the photon pairs were reevaluated using the fitted energy values. The mass resolution for the Higgs signal after the kinematic fit was found to be 1 GeV/c^2.

4 Results

From the results in table 1, according to the SM, no evidence for unexpected phenomena has been found. Model-independent limits at 95% Confidence Level (CL) on the cross-sections were derived for the different topologies studied at the centre-of-mass energies of 161 GeV, 172 GeV and 183 GeV. The limits were obtained using a Poisson distribution with background [33] and taking into account the mass resolution information for each topology.

The 95% CL upper limits on $\sigma(e^+e^- \to H\gamma) \times BR(H \to b\bar{b})$, $\sigma(e^+e^- \to Hq\bar{q}) \times BR(H \to \gamma\gamma)$ and $\sigma(e^+e^- \to H\gamma) \times BR(H \to \gamma\gamma)$ are displayed in figure 4 (a), (b) and (c) respectively. The limits obtained depend on the efficiency for the detection of the final state particles. For Higgs boson masses above the kinematic limit, the cross-sections correspond to the production of a virtual Higgs boson. For this reason the signal efficiency does not drop to zero at threshold. Nevertheless, when the model-independent limits are converted into a specified model, limits obtained for masses above the threshold will be

[1] $\mathrm{mod}(\phi, 15°) = 7.5° \pm 1.0°$, for more details see [9,10]

[2] The χ^2 parameter was defined as $\chi^2 = \frac{1}{3}\sum_{i=1,3}\left(\frac{p_i^{calc} - p_i^{meas}}{\sigma_i}\right)^2$ p_i^{meas} are the measured momenta or energies and p_i^{calc} are the momenta calculated from the kinematic constraints. σ_i, is defined in reference [32] for the three photon topology.

much weaker since the Higgs production cross-section would have to be very large for its virtual states to be seen.

Limits on the anomalous couplings were computed for a centre-of-mass energy of 183 GeV. They were set assuming three different scenarios:

In the first scenario each f_i parameter was considered independently by setting all the others to zero. Limits on each f_i/Λ^2 parameter were set as a function of the Higgs boson's mass (figure 5). The $\gamma\gamma\gamma$ analysis contributes to set exclusion limits on the values of $|f_{BB}/\Lambda^2|$ and $|f_{WW}/\Lambda^2|$ for Higgs boson masses up to 145 GeV/c^2. The $q\bar{q}\gamma\gamma$ analysis leads to tighter limits on f_{BB} for masses M_H up to 80 GeV/c^2. The $b\bar{b}\gamma$ cross-section has a weak dependence on f_{BB} and f_{WW} and the analysis of this process does not improve the limits on these two parameters.

When f_{BB} and f_{WW} are zero, $H \to \gamma\gamma$ has a negligible rate so the $\gamma\gamma\gamma$ and $q\bar{q}\gamma\gamma$ processes do not contribute to set limits on other parameters. In this case $H \to b\bar{b}$ is the dominant decay and limits on f_B and f_W may be obtained for M_H up to 100 GeV/c^2 (figures 5 (c) and (d)).

Also shown in figure 5 (c) are the limits obtained on the anomalous TGC parameters by the direct measurements of WW production [34] (dashed-dotted horizontal lines). As mentioned in section 2, f_B/Λ^2 and f_W/Λ^2 contribute also to the TGCs, and the resulting constraints from the $b\bar{b}\gamma$ analysis give indirect limits on the deviations from the SM trilinear gauge boson couplings vertices. The anomalous $WW\gamma$ and WWZ dipole like couplings and the WWZ charge like couplings are defined as:

$$\Delta k_\gamma = \frac{M_W^2}{2}\frac{(f_B + f_W)}{\Lambda^2}, \qquad \Delta k_Z = \frac{M_W^2}{2}\frac{(f_B.\tan^2\theta_W + f_W)}{\Lambda^2}, \qquad \Delta g_1^Z = \frac{M_Z^2}{2}\frac{f_W}{\Lambda^2} \tag{6}$$

In the case in which only f_B is different from zero, Δk_γ is proportional to f_B/Λ^2 and Δg_1^Z is zero, assumptions used in the TGC direct limit for Δk_γ. In this case the limit obtained with the $b\bar{b}\gamma$ analysis improves the direct limit of masses M_H up to 100 GeV/c^2.

In the second scenario, all f_i except f_{BB} and f_{WW} (which directly contribute to the decay $H \to \gamma\gamma$) were assumed to be negligible. In this scenario, the derived 95% CL cross-section upper limits were used to exclude regions in the f_{WW} vs f_{BB} plane. The contour plots of the limits obtained from the $b\bar{b}\gamma$, $q\bar{q}\gamma\gamma$ and $\gamma\gamma\gamma$ analyses are displayed in figure 6 for $M_H = 80$ GeV/c^2 and $M_H = 120$ GeV/c^2. For $M_H = 80$ GeV/c^2, each final state contributes to exclude particular regions in the f_{WW} vs f_{BB} plane. For $M_H = 120$ GeV/c^2 the limits derived using the $\gamma\gamma\gamma$ final state are clearly stronger than those from the hadronic final states analysis.

In the third scenario the simplest assumption was made. All f_i's have a strength of the same order and are set to $f_i = F$. The $q\bar{q}\gamma\gamma$ cross-section shows a clear asymmetry between positive and negative values of F/Λ^2, due to the interference between the anomalous and standard HZZ coupling (figure 1(c)). For the other final states there is no such interference, as in the SM there is no tree-level vertex for the Higgs boson production with a photon. For the $b\bar{b}\gamma$ the dependence on the F/Λ^2 parameter is weaker since the anomalous coupling is only present in the production vertex. In this scenario, limits on F/Λ^2 as a function of the Higgs boson mass were derived (figure 7). Stronger constraints on F/Λ^2 come from the three-photon analysis results, and are of the order $\pm$ 35 TeV^{-2} for $M_H < 100$ GeV/c^2. The $q\bar{q}\gamma\gamma$ results improve the $\gamma\gamma\gamma$ limit if $M_H < 90$ GeV/c^2 for negative values of F. If F is positive, the interference between anomalous and SM HZZ

couplings is destructive, therefore the limit obtained is not as strong. The $q\bar{q}\gamma\gamma$ cross-section decreases above $M_H = 90$ GeV/c^2, which corresponds to the kinematic limit for HZ production. In the mass region analysed, the $b\bar{b}\gamma$ final state does not improve the limits.

5 Summary

DELPHI data corresponding to integrated luminosities of 47.7 pb^{-1}, 10.1 pb^{-1} and 9.7 pb^{-1} at the centre-of-mass energies of 183 GeV, 172 GeV and 161 GeV respectively have been analysed and a search for the Higgs boson in final states $b\bar{b}\gamma$, $q\bar{q}\gamma\gamma$ and $\gamma\gamma\gamma$ performed. No evidence of unexpected phenomena has been found. Model-independent upper limits on the cross-sections of these processes were derived at 95 % CL as a function of the Higgs mass. The cross-section upper limits have been used to derive limits on contributions from operators which could give rise to anomalous Higgs to gauge boson couplings and trilinear gauge boson couplings.

Acknowledgements

We would like to thank J.C.Romão for very interesting and long discussions, S.F.Novaes for his cooperation in cross checking our results and V.Ilyin for his assistance in the use of the CompHEP and LanHEP packages.
We are greatly indebted to our technical collaborators, to the members of the CERN-SL Division for the excellent performance of the LEP collider, and to the funding agencies for their support in building and operating the DELPHI detector.
We acknowledge in particular the support of
Austrian Federal Ministry of Science and Traffics, GZ 616.364/2-III/2a/98,
FNRS–FWO, Belgium,
FINEP, CNPq, CAPES, FUJB and FAPERJ, Brazil,
Czech Ministry of Industry and Trade, GA CR 202/96/0450 and GA AVCR A1010521,
Danish Natural Research Council,
Commission of the European Communities (DG XII),
Direction des Sciences de la Matière, CEA, France,
Bundesministerium für Bildung, Wissenschaft, Forschung und Technologie, Germany,
General Secretariat for Research and Technology, Greece,
National Science Foundation (NWO) and Foundation for Research on Matter (FOM), The Netherlands,
Norwegian Research Council,
State Committee for Scientific Research, Poland, 2P03B06015, 2P03B03311 and SPUB/P03/178/98,
JNICT–Junta Nacional de Investigação Científica e Tecnológica, Portugal,
Vedecka grantova agentura MS SR, Slovakia, Nr. 95/5195/134,
Ministry of Science and Technology of the Republic of Slovenia,
CICYT, Spain, AEN96–1661 and AEN96-1681,
The Swedish Natural Science Research Council,
Particle Physics and Astronomy Research Council, UK,
Department of Energy, USA, DE–FG02–94ER40817.

References

[1] K. Hagiwara, R. Szalapski, D. Zeppenfeld, Phys. Lett. **B318** (1993) 155
[2] A. Barroso, J. Pulido, J.C. Romão, Nucl. Phys. **B267** (1986) 509
[3] A. Abbasabadi et al., Phys. Rev. **D52** (1995) 3919
[4] J. Ellis, M.K. Gaillard and D.V. Nanopoulos, Nucl. Phys. **B106** (1976) 292,
A.I. Vainshtein et al., Sov. J. Nucl. Phys. **30** (1979) 711
[5] G. Gamberini, G.F. Giudice, G. Ridolfi, Nucl. Phys. **B292** (1987) 237
[6] R. Bates, John N.Ng, P. Kalyniak, Phys. Rev **D34** (1986) 172
[7] O.J.P.Eboli, M.C.Gonzalez-Garcia, S.M.Lietti and S.F.Novaes, Phys. Lett. **B434** (1998) 340
[8] OPAL Coll.,K. Ackerstaff et al., Phys. Lett. **B437** (1998) 218
[9] DELPHI Coll., P. Aarnio et al., Nucl. Instr. and Meth. **A303** (1991) 233
[10] DELPHI Coll., P. Abreu et al., Nucl. Instr. and Meth. **A378** (1996) 57
[11] P. Higgs, Phys. Lett. **12** (1964) 132,
P. Higgs, Phys. Rev. Lett. **13** (1964) 508,
P. Higgs, Phys. Rev. **145** (1966) 1156,
F. Englert and R. Brout, Phys Rev. Lett. **13** (1964) 321,
G.S. Guralnik, C.R. Hagen, T.W.B. Kibble, Phys Rev. Lett. **13** (1964) 585
[12] "Physics at LEP2", ed. G.Altarelli, T. Sjöstrand, F.Zwirner, CERN 96-01 (1996)
[13] Z. Kunszt, W.J. Stirling, "The Standard Model Higgs at LHC: Branching Ratios and Cross-Sections", CERN 90-10, ECFA 90-133, Vol. 2 (1990)
[14] "Lower bound for the Standard Model Higgs boson mass from combining the results of the four LEP experiments", CERN-EP/98-046,
ALEPH Coll., R. Barate et al., Phys. Lett. **B412** (1997) 155,
DELPHI Coll., P.Abreu et al., Eur. Phys. J. **C2** (1998) 1,
L3 Coll., M. Acciarri et al., Phys. Lett. **B411** (1997) 373,
OPAL Coll., K. Ackerstaff, Eur. Phys. J. **C1** (1998) 425
[15] P.J. Franzini et al., Z Physics at LEP 1, CERN 89-08 (1989)
[16] A. Djouadi,"Decays of the Higgs boson", hep-ph/9712334
[17] K. Hagiwara, S. Ishihara, R. Szalapski, D. Zeppenfeld, Phys. Rev. **D48** (1993) 2182
[18] T. Sjöstrand, Comp. Phys. Comm. **82** (1994) 74,
T. Sjöstrand, Pythia 5.7 and Jetset 7.4, Cern-TH/7112-93
[19] E.E. Boos, M.N. Dubinin, V.A. Ilyin, A.E. Pukhov, V.I. Savrin, Preprint INP MSU 94-36/358 and SNUCTP 94-116 (1994); hep-ph/9503280,
P.A. Baikov et al., in Proc. X Workshop QFTHEP-95 (Zvenigorod, September 1995), ed. B. Levtchenko and V. Savrin (MSU, Moscow, 1996) p.101; hep-ph/9701412
[20] A.V. Semenov, "LanHEP- a package for automatic generation of Feynman rules in gauge models", INP-MSU-96-24-431 and hep-ph/9608488
[21] J.C. Romão and S. Andringa, "Vector Boson Decays of the Higgs", hep-ph/9807536
[22] F.A. Berends, W. Hollik and R. Kleiss, Nucl. Phys. **B304** (1988) 712
[23] F.A. Berends, R. Pittau, R. Kleiss, Comp. Phys. Comm. **85** (1995) 437
[24] S. Nova, A. Olchevski and T. Todorov, "TWOGAM, a Monte Carlo event generator for two photon physics", DELPHI Note 90-35 PROG 152
[25] F.A. Berends, P.H. Daverveldt, R. Kleiss, Comp. Phys. Comm. **40** (1986) 271
[26] D. Karlen, Nucl. Phys. **B289** (1987) 23
[27] F. Berends and R. Kleiss, Nucl. Phys. **B186** (1981) 22
[28] S. Catani et al., Phys. Lett. **B269** (1991) 432
[29] DELPHI Coll., P. Abreu et al., Eur. Phys. J. **C2** (1998) 581

[30] DELPHI Collaboration, P. Abreu et al., Zeit. Phys. **C70** (1996) 531;
G. Borisov and C. Mariotti, NIM **A372** (1996) 181.
[31] DELPHI Coll., P. Abreu et al., Phys. Lett. **B433** (1998) 429
[32] DELPHI Coll., P. Abreu et al., Phys. Lett. **B380** (1996) 480,
DELPHI Coll., P. Abreu et al., Zeit. Phys. **C53** (1992) 41
[33] Particle Data Group, R. M. Barnett et al., Phys.Rev. **D54** (1996) 1
[34] T.J.V. Bowcock et al., "Measurement of Trilinear Gauge Boson Couplings WWV ($\mathrm{V} \equiv \gamma, Z$) in e^+e^- Collisions at 183 GeV", DELPHI 98-94 CONF 162

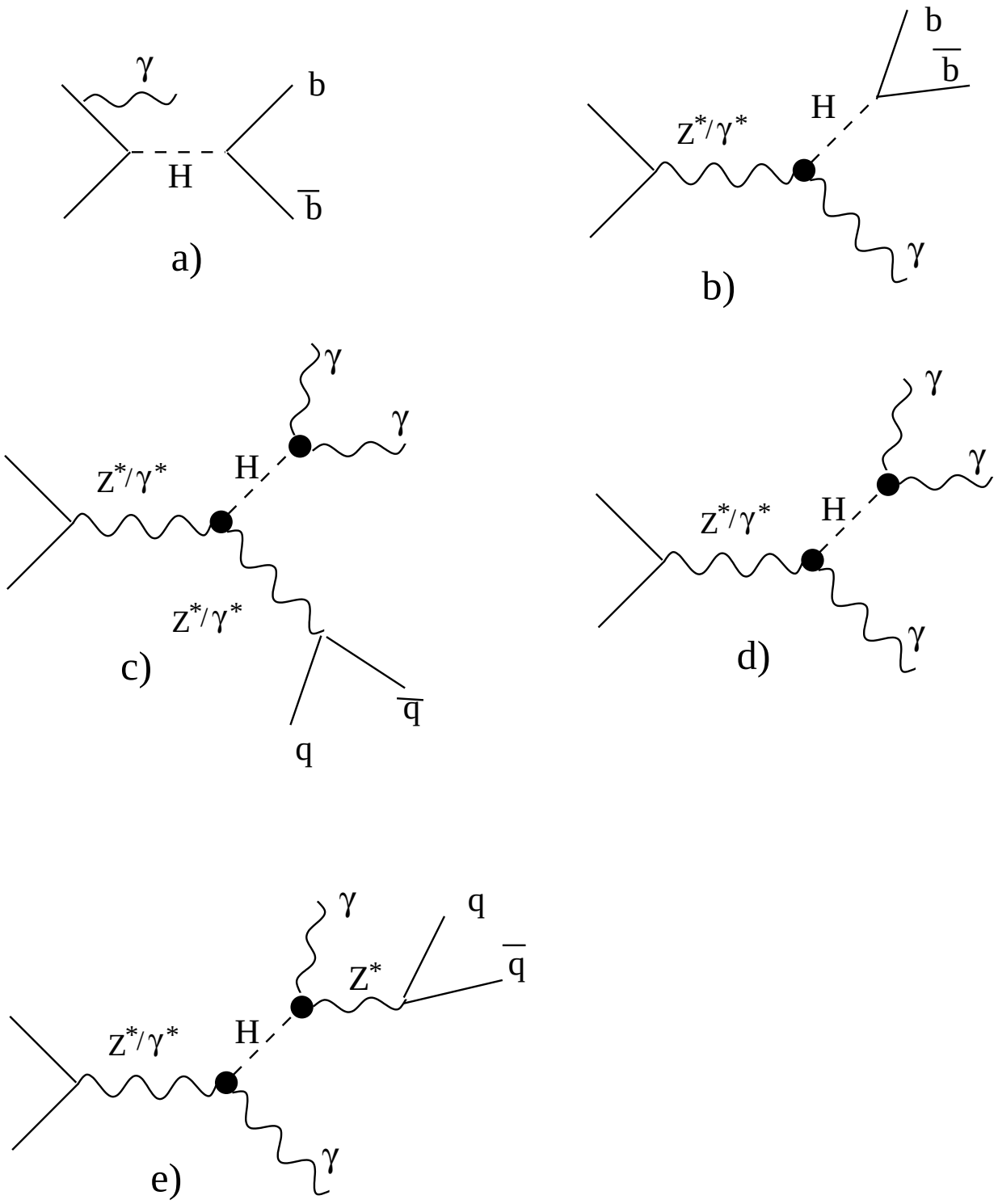

Figure 1: Feynman diagrams for the Higgs production at LEP. The analysed processes are (b), (c) and (d).

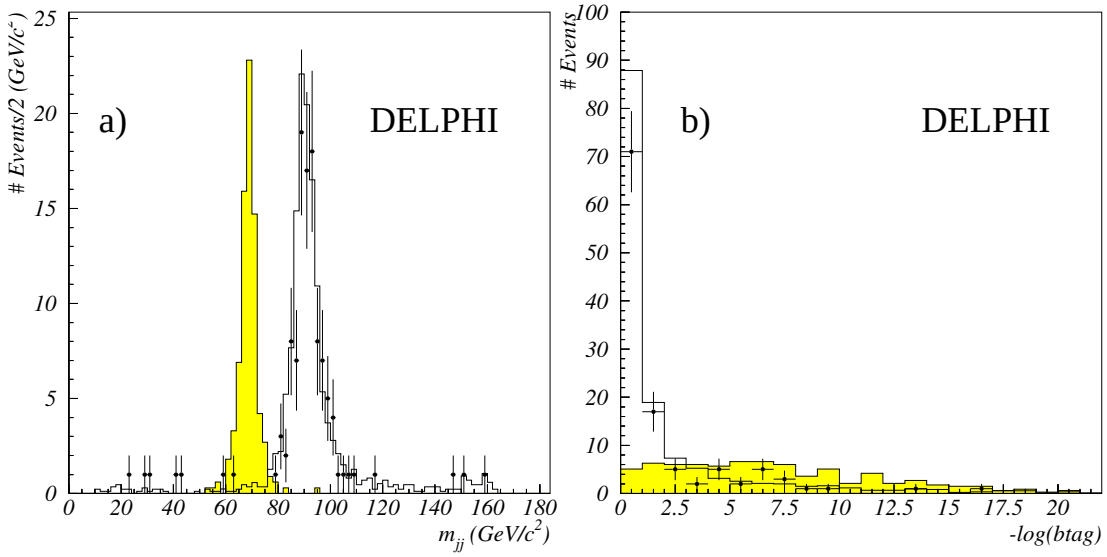

Figure 2: a) Fitted jet-jet invariant mass and b) negative logarithm of the b-tagging probability, for the $b\bar{b}\gamma$ topology corresponding to the 183 GeV data sample(dots). The white histograms correspond to the simulated background and the shaded histograms to a 70 GeV/c^2 Higgs boson signal (the normalization is arbitrary). Selection level 2 has been applied both to data and simulation.

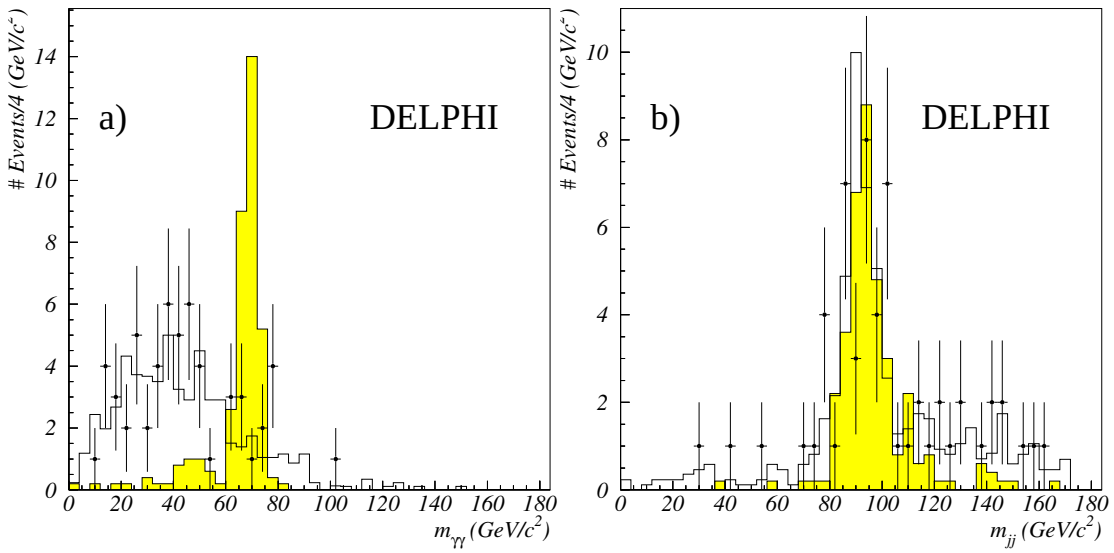

Figure 3: a) Fitted $\gamma\gamma$ and b) jet-jet invariant mass spectra corresponding to the $q\bar{q}\gamma\gamma$ topology for the 183 GeV selected sample (dots). The white histograms represent the simulated background distributions and the shaded histograms correspond to the $\gamma\gamma$ and jet-jet invariant mass distributions for a simulated 70 GeV/c^2 Higgs boson signal (the normalization is arbitrary). Selection level 1 has been applied both to data and simulation.

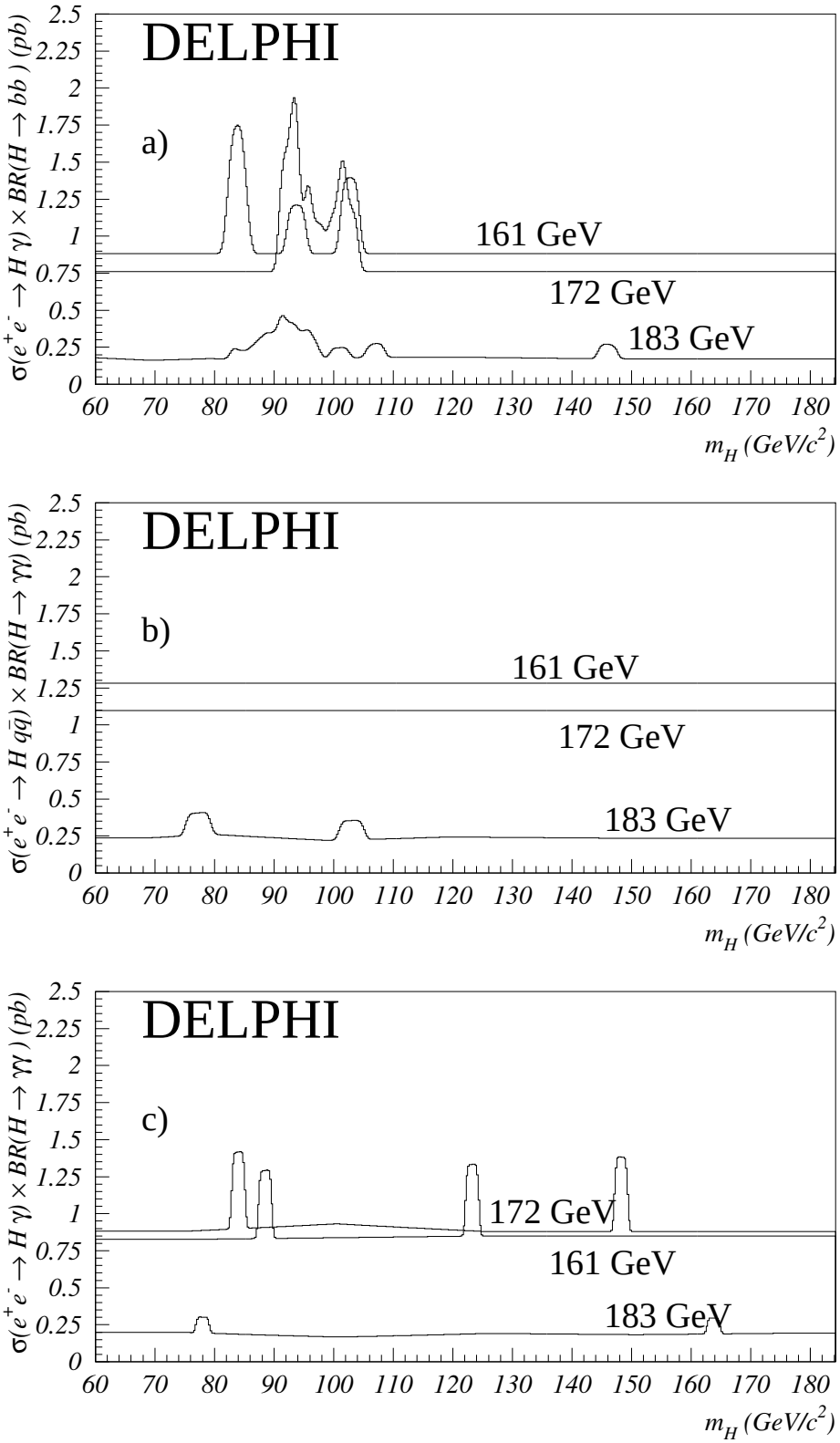

Figure 4: 95%CL upper limits on : a) $\sigma(e^+e^- \to H\gamma) \times BR(H \to b\bar{b})$, b) $\sigma(e^+e^- \to Hq\bar{q}) \times BR(H \to \gamma\gamma)$, c) $\sigma(e^+e^- \to H\gamma) \times BR(H \to \gamma\gamma)$, as a function of the Higgs boson mass for the centre-of-mass energies of 161, 172 and 183 GeV.

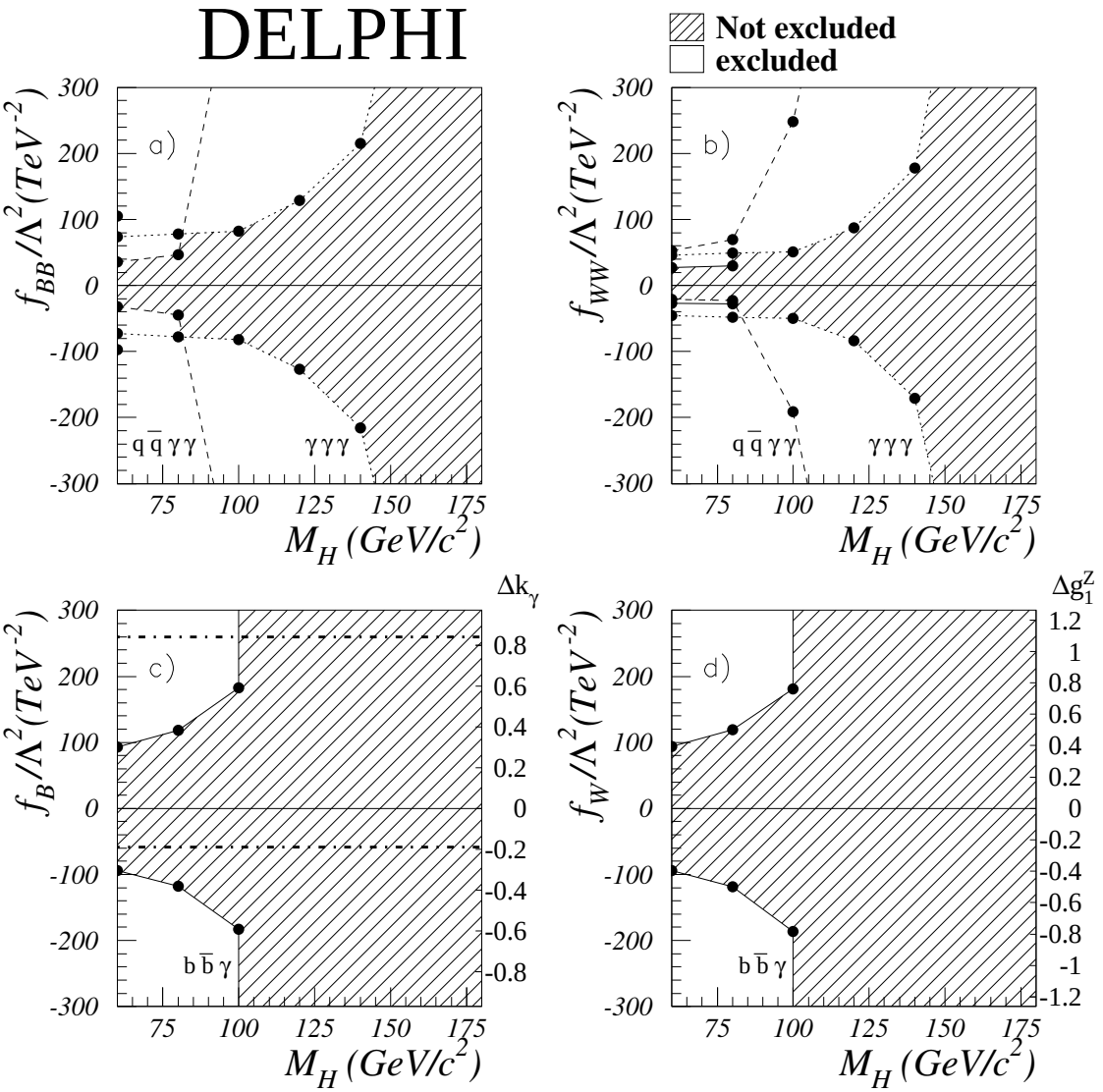

Figure 5: 95% CL limits on each f_i/Λ^2 parameter as a function of M_H, when other f_i are set to zero. The full, dashed and dotted lines correspond to the $b\bar{b}\gamma$, $q\bar{q}\gamma\gamma$ and $\gamma\gamma\gamma$ analysis, respectively. Only $b\bar{b}\gamma$ contributes to set limits on f_B and f_W. In c) and d) the right hand scales correspond to TGC parameters (Δk_γ and Δg_1^Z) and the dashed-dotted horizontal line is the 95% CL limit on Δk_γ from TGC measurements.

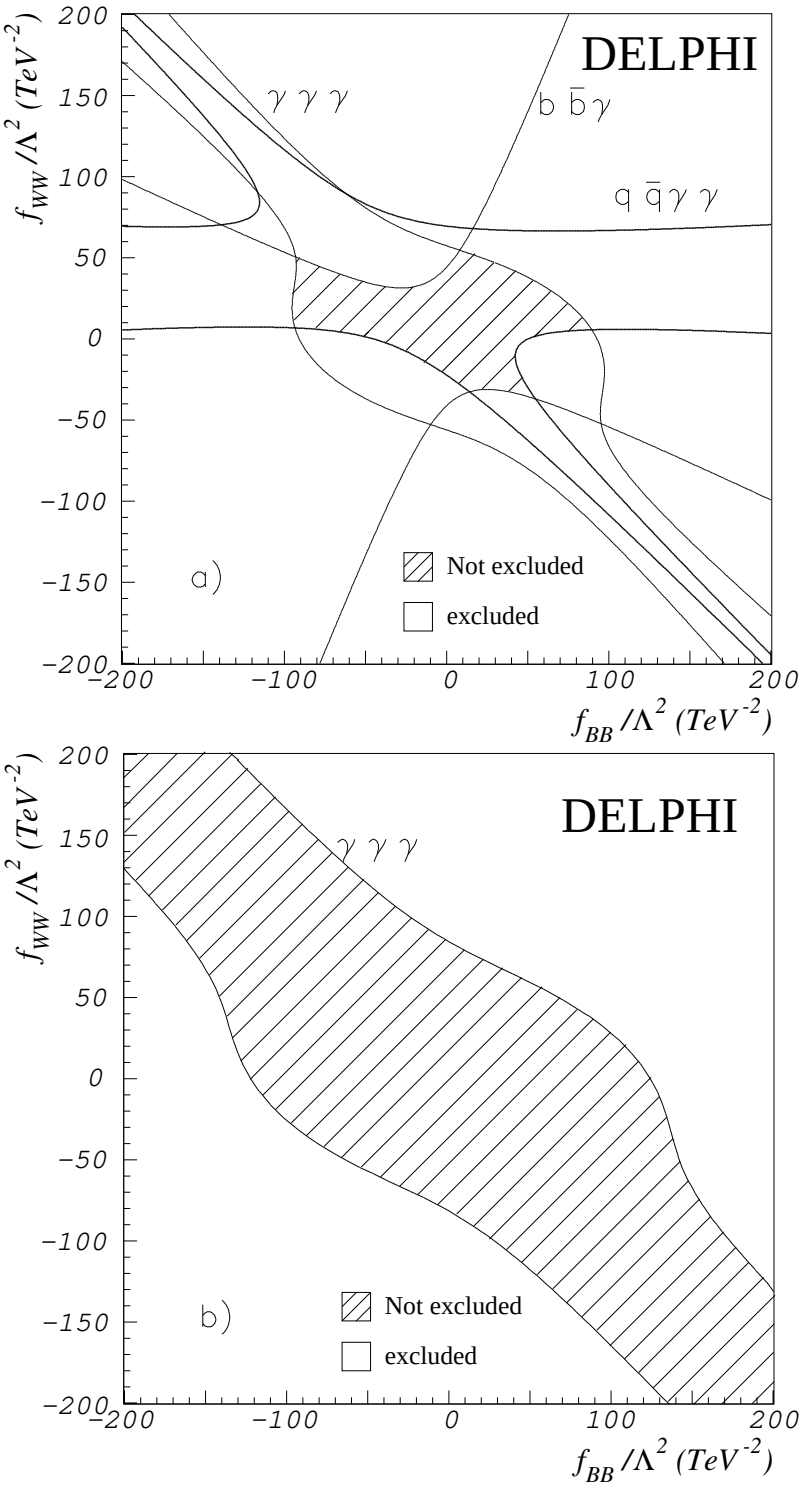

Figure 6: 95% CL exclusion regions in the $f_{BB} \times f_{WW}$ plane (a) for $M_H = 80$ GeV/c^2, (b)for $M_H = 120$ GeV/c^2, corresponding to a centre-of-mass energy of 183 GeV. The contour lines correspond to the upper limits on the cross-section of the processes $b\bar{b}\gamma$, $q\bar{q}\gamma\gamma$ and $\gamma\gamma\gamma$. For $M_H = 120$ GeV/c^2, the limits derived using the hadronic channels are outside the region of $f_{BB} \times f_{WW}$ considered.

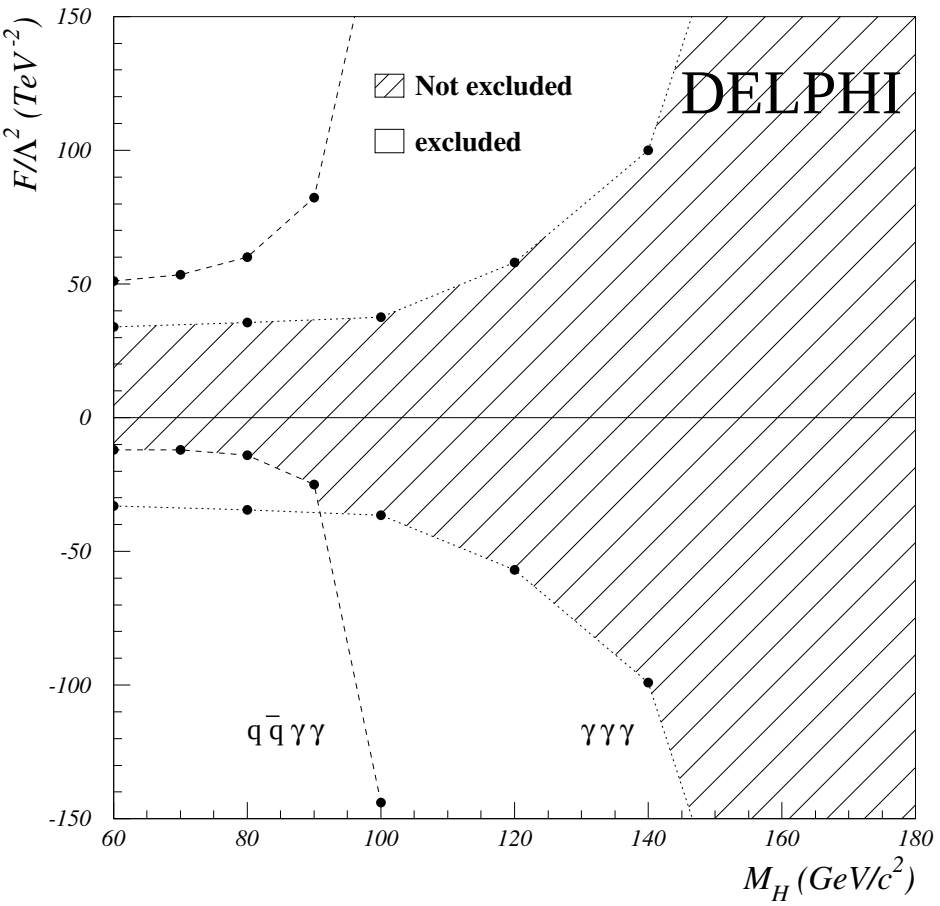

Figure 7: 95% CL limits on F/Λ^2 as a function of the Higgs boson mass, from the 183 GeV analysis. The dotted line corresponds to the $\gamma\gamma\gamma$ and the dashed line to the $q\bar{q}\gamma\gamma$ analysis.